Journal of Engineering Physics and Thermophysics, Vol. 68, No. 2, 1995

DATABANK ON THERMODYNAMIC AND OPTICAL PROPERTIES OF PLASMA

G. S. Romanov, Yu. A. Stankevich, L. K. Stanchits, and K. L. Stepanov

UDC 533.95:537:56

Methods of evaluation of thermodynamic and optical properties of multicomponent gases within a wide range of conditions are discussed. A databank on component composition, thermodynamic functions, spectral and group absorption coefficients, and Planck and Rosseland mean free paths of radiation for plasmas of air, water, silicon dioxide, and the Martian atmosphere (0.965 CO_2 + 0.035 N_2) is composed based on calculations.

Introduction. Data on thermophysical and optical properties of matter are required in solving a number of pressing problems of radiation gas dynamics and plasmadynamics connected with investigations of high-temperature phenomena (entry of space vehicles and meteorite bodies into the atmosphere of planets [1], powerful explosion and high-speed impact [2, 3], interaction of laser and wide-band radiation with matter [4, 5], high-current radiating discharges [6], etc.), and therefore creation of databanks on thermodynamic and optical properties of gases within a wide range of temperatures, densities (pressures), and energies of quanta proves to be of importance. The use of actual opticophysical parameters of matter makes it possible to study these phenomena not only at a qualitative but also at a quantitative level, which is required in the development of new technological processes with a high energy concentration. Presently, data of this type exist for air [7-12], several metals and dielectrics [13-18], a series of noble gases [19, 20], and mixtures [21].

In the present work we consider methods and results of systematic calculations of thermodynamic properties, the composition, and spectral and averaged absorption coefficients of air, water, silicon dioxide, and the Martian atmosphere. The temperature range under consideration $0.1-10^3$ eV includes the molecular state of matter, dissociated gas, and low-temperature and multicharge plasma, including complete ionization. The density range $\delta = \rho/\rho_0 = 10^{-6}-10^1$ (ρ_0 corresponds to a concentration of original particles equal to the Loschmidt number $N_L = 2.687 \cdot 10^{19}$ cm^{-3}) makes it possible to carry out substantiated calculations within the framework of the tested approximation of a weakly nonideal equilibrium plasma and includes the region of parameters most interesting for applications. The spectral range of energy of quanta for which the absorption coefficients are determined is $\varepsilon = 10^{-1}-10^4$ eV. The wide spectral range and the detailed resolution of the spectrum provide the possibility of investigating problems of radiation transfer within spectral and multigroup approximations.

The substantial difference of the results obtained in the present work from those presented in a number of publications (e.g., [21]) is attributable to taking into account molecular absorption and the effect of transitions in the discrete spectrum of atoms and ions on the total absorption coefficient. Absorption of radiation by molecules dominates at low temperatures and turns out to be noticeable at $T \geq 1$ eV as well with increase in density. Taking into account the contribution of the line spectrum is particularly important for multicharge plasma, in which the radiation of spectral lines is the main mechanism of radiative losses [22].

Calculations of composition, thermodynamic functions, and absorption coefficients were carried out within a temperature scale that makes it possible to provide a rather detailed description of the change in the state of the medium in dissociation and ionization processes. For this purpose, at $T < 20{,}000$ K the step in the temperature was chosen equal to 500 K within the range 1000–6000 K, 1000 K for $6000 < T < 10{,}000$ K, and 2000 K within the region $10{,}000 < T < 20{,}000$ K. At $T \geq 1.99$ eV a logarithmic temperature scale with a step of $\Delta \log T = 0.1$

Academic Scientific Complex "A. V. Luikov Institute of Heat and Mass Transfer of the Academy of Sciences of Belarus," Minsk, Belarus. Translated from Inzhenerno-Fizicheskii Zhurnal, Vol. 68, No. 2, pp. 291-305, March-April, 1995. Original article submitted December 8, 1993.

1062-0125/95/6802-0255$12.50

(28 isotherms beginning with $T = 1.99$ eV) was used. The step in the density was chosen to be $\Delta \log \delta = 0.5$ (15 isochores beginning with $\delta = 10^{-6}$).

In evaluation of spectral absorption coefficients the contributions of bound-bound, free-free, and bound-free transitions were summed up. The absorption coefficient in the continuum, the integral line strengths, and the broadening constants were calculated separately. These data make it possible to determine mean absorption coefficients within spectral ranges with reasonable accuracy. The spectral groups over which the absorption coefficients were averaged were chosen as follows. To provide matching with data from [9] the calculations within the range $\varepsilon \leq 17.354$ eV were performed using 560 groups with a step of 250 cm^{-1}, i.e., the step of averaging is 0.03099 eV. Beginning with 17.354 eV a logarithmic scale was used on which the averaging step was given by the formula $\Delta\varepsilon = \varepsilon_0 \cdot 10^{(i-560)/500}$, where $\varepsilon_0 = 8.010259 \cdot 10^{-2}$ eV. Hence, the total number of spectral ranges was 1941.

In composing a databank on optical properties of air the results from [9] (the temperature range $T < 20{,}000$ K) were supplemented with data obtained in the present work for energies $\varepsilon \geq 17.354$ eV and for the temperature range $1.99 \leq T \leq 10^3$ eV.

Thermodynamic Properties. Let us consider briefly the methods of evaluation of thermodynamic parameters. Equilibrium concentrations of particles were determined based on the law of acting masses for the leading components in the gas. For example, in air they are N_2, O_2, and NO molecules, N_2^+, O_2^+, and NO^+ molecular ions, N, O, and Ar atoms and their ions, and electrons. For the reactions

$$N_2 + M \Leftrightarrow N + N + M, \quad O_2 + M \Leftrightarrow O + O + M, \quad NO + M \Leftrightarrow N + O + M,$$

$$N + O \Leftrightarrow NO^+ + e, \quad N + N \Leftrightarrow N_2^+ + e, \quad O + O \Leftrightarrow O_2^+ + e \tag{1}$$

the equations of chemical equilibrium are as follows:

$$(n_N)^2 = F_1 n_{N_2}, \quad (n_O)^2 = F_2 n_{O_2}, \quad n_N n_O = F_3 n_{NO},$$

$$n_e n_{NO^+} = F_4 n_N n_O, \quad n_e n_{N_2^+} = F_5 (n_N)^2, \quad n_e n_{O_2^+} = F_6 (n_O)^2. \tag{2}$$

The concentration of ions of successive degrees of ionization was calculated using the Saha system of equations within the annular Debye approximation [23]

$$\frac{n_{i+1}\, n_e}{n_i} = 2\, \frac{\Sigma_{i+1}}{\Sigma_i} \left(\frac{4\pi m k T}{h^2} \right)^{3/2} \exp\left(- \frac{I_i - \Delta I_i}{kT} \right). \tag{3}$$

The constants in (2) and (3) are determined by the combination of atomic-molecular parameters of the components. Their values, in particular, the energy spectra, the statistical weights of levels, rotational and vibrational constants, and dissociation and ionization energies, were given according to [24-27].

The decrease in the ionization potential induced by the Coulomb interaction of the particles is as follows:

$$\frac{\Delta I_i}{kT} = \ln \frac{(1 + \gamma/2)\, [1 + (z_i + 1)^2 \gamma/2\,]}{(1 + z_i^2\, \gamma/2)}, \tag{4}$$

where z_i is the charge of an ion of the i-th type ($i = 1$ for neutral particles). The parameter γ is determined as the positive root of the equation

$$\gamma^2 = \left(\frac{e^2}{kT} \right)^3 4\pi \sum \frac{n_i z_i^2}{1 + z_i^2\, \gamma/2}. \tag{5}$$

For weakly nonideal plasma the quantity γ coincides with the usual nonideality parameter

$$\Gamma = \frac{e^2}{kTr_D} = \left(\frac{e^2}{kT} \right)^{3/2} \left\{ 4\pi \left(\sum n_i z_i^2 + n_e \right) \right\}^{1/2}. \tag{6}$$

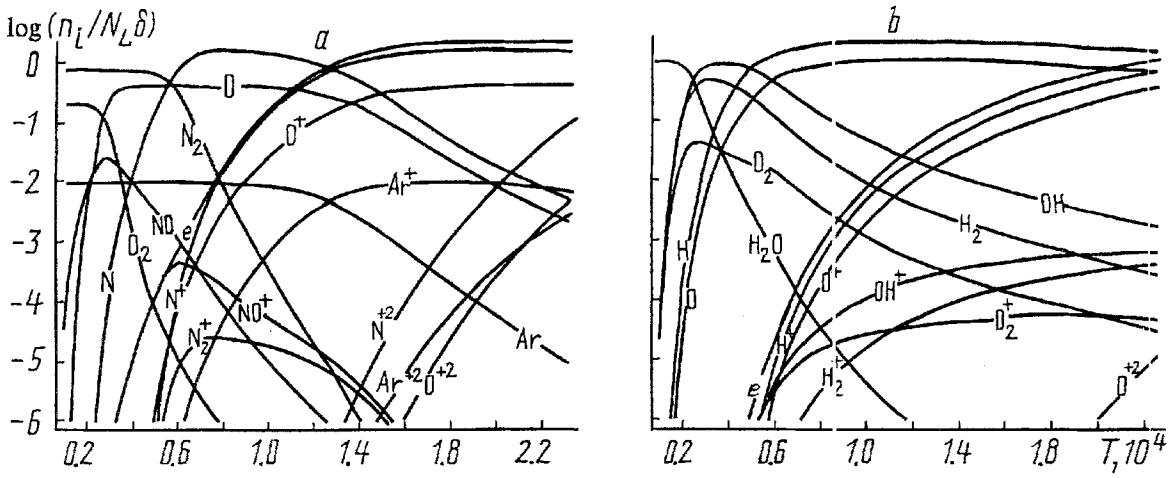

Fig. 1. Composition of air plasma at $\delta = 10^{-3}$ (a) and H_2O plasma at $\delta = 1$ (b) as a function of the temperature T.

Statistical sums for atom and ions were calculated using the Planck-Larkin formula

$$\sum_i = \sum g_{ij} \exp(-E_{ij}/kT)\, W_{ij},$$

$$W_{ij} = 1 - \left(1 + \frac{I_i - E_{ij}}{kT}\right) \exp\left(\frac{E_{ij} - I_i}{kT}\right). \tag{7}$$

Thermodynamic functions (density, pressure, specific internal energy, effective adiabat exponent) were found from the formulas

$$\rho = 1.67 \cdot 10^{-24} \sum n_i A_i, \quad P = kT \sum n_i - P_k,$$

$$E = \frac{3kT}{2\rho} \sum n_i + \frac{kT}{2\rho} \sum_m n_m q_m + \frac{1}{\rho} \sum_m n_m \sum_\nu \frac{h\omega_\nu g_\nu}{\exp(h\omega_\nu/kT) - 1} + \frac{1}{\rho} \sum n_i (Q_i + \bar{\varepsilon}_i) - E_k,$$

$$\gamma_{ef} = 1 + \frac{P}{\rho E}. \tag{8}$$

Here A_i is the atomic weight, Q_i and $\bar{\varepsilon}_i$ are the energy of formation and the mean energy of excitation of the particles, respectively; q_m and g_ν are the number of rotational degrees of freedom of a molecule and the statistical weight of its vibrational mode, respectively. The Coulomb corrections to the thermodynamic functions are as follows:

$$P_k = \frac{kT\chi^3}{24\pi}, \quad E_k = \frac{kT\chi^3}{8\pi\rho}, \quad \chi = \gamma \frac{kT}{e^2}. \tag{9}$$

In calculations of the composition of silicon dioxide vapor, owing to the high heat of evaporation, we considered its equilibrium with the condensed phase, and therefore at temperatures less than 6000 K the gas density was bounded above by the vapor density at the boundary of the two-phase region. The curve $\rho(T)$ that bounds the two-phase region was calculated according to [28].

Let us present several illustrations of the calculations performed. The dependence of the component composition of low-temperature plasma on T is shown in Fig. 1. Here ratios of the concentration of the particles to the quantity δN_L are shown for air and water. Thus, their sum at $T \to 0$ equals unity. With increase in T when dissociation and ionization occur, the total concentration increases.

The dependence of the parameters of plasma on its density is presented in Table 1, where on the example of the Martian atmosphere the values of P (dyn/cm^2), E (erg/g), effective adiabatic exponent γ_{ef}, mean molecular weight M, and concentrations $\bar{n}_i = n_i/\delta N_L$ are presented for two isotherms. It is clear that the temperature range within which molecules are present increases substantially with density, and in this case the thermodynamic and optical properties depend on the ever-growing number of components. Note the role of molecular ions that determine

TABLE 1. Dependence of Parameters of the Martian Atmosphere (0.965 CO_2+0.035 N_2) on Density

Характеристика	δ			
	1,00—06	1,00—04	1,00—02	1,00+00
		T=3000 K		
P	2,18+01	2,09+03	1,57+05	1,25+07
E	1,43+11	1,34+11	7,92+10	4,51+10
γ_{ef}	1,08+00	1,08+00	1,10+00	1,14+00
M	2,21+01	2,31+01	3,08+01	3,88+01
e	9,76—07	2,81—07	3,91—08	3,08—09
CO_2	2,69—04	2,25—02	3,15—01	7,37—01
CO	9,65—01	9,43—01	6,50—01	2,28—01
N_2	3,43—02	3,24—02	2,99—02	3,15—02
O_2	7,82—04	5,72—02	2,36—01	1,05—01
NO	6,27—04	5,21—03	1,02—02	6,96—03
N	7,80—04	7,58—05	7,29—06	7,48—07
O	9,63—01	8,23—01	1,67—01	1,12—02
C	2,27—07	2,60—09	8,81—11	4,64—12
NO^+	9,75—07	2,81—07	3,91—08	3,08—09
		T=30 000 K		
P	1,07+03	9,33+04	6,99+06	5,44+08
E	4,93+12	3,75+12	2,12+12	1,43+12
γ_{ef}	1,11+00	1,13+00	1,17+00	1,20+00
M	4,53+00	5,16+00	6,82+00	8,40+00
e	6,62+00	5,45+00	3,40+00	2,20+00
CO	4,11—28	3,59—18	1,04—10	2,06—05
N_2	8,15—31	4,99—21	1,58—13	2,60—08
O_2	1,00—26	2,79—17	1,51—10	1,71—05
C_2	2,10—30	5,74—20	9,00—12	3,10—06
N	9,79—11	7,66—07	4,30—04	1,75—02
O	1,44—08	7,62—05	1,77—02	5,96—01
C	1,32—10	2,18—06	2,73—03	1,61—01
N^{+1}	6,45—05	6,19—03	5,88—02	5,23—02
O^{+1}	7,11—03	4,60—01	1,81+00	1,33+00
C^{+1}	1,44—04	2,91—02	6,17—01	7,93—01
N^{+2}	5,36—02	6,36—02	1,07—02	2,49—04
O^{+2}	1,84+00	1,47+00	1,03—01	1,98—03
C^{+2}	3,66—01	9,17—01	3,45—01	1,16—02
N^{+3}	1,63—02	2,42—04	7,51—07	4,47—10
O^{+3}	8,64—02	8,62—04	1,11—06	5,47—10
C^{+3}	5,98—01	1,87—02	1,29—04	1,11—07

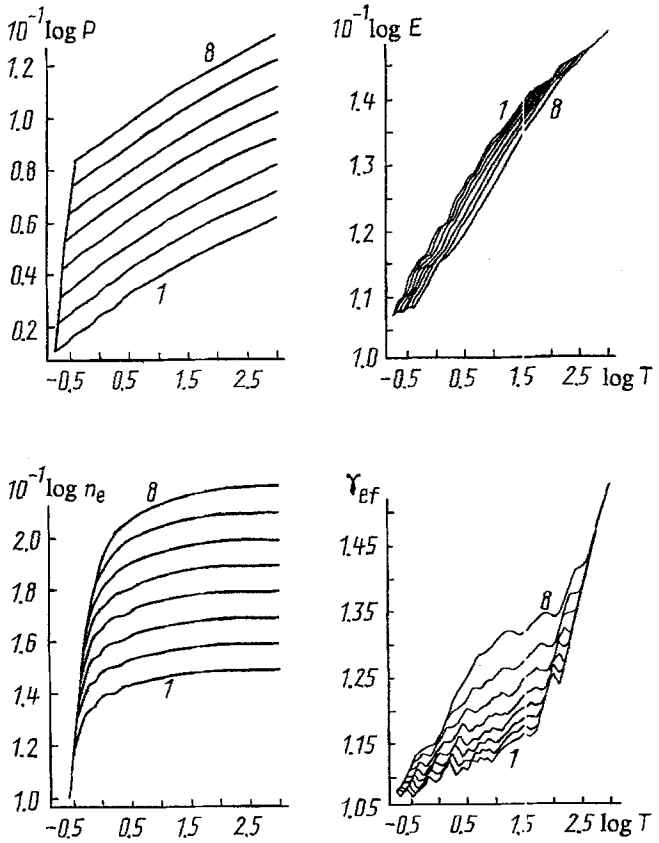

Fig. 2. Thermodynamic properties of SiO_2. log *P*, dyn/cm^2; log *E*, erg/g; log n_e, cm^{-3}; log *T*, eV.

TABLE 2. Density and Pressure of Saturated SiO_2 Vapor as a Function of Temperature

T, K	2000	2500	3000	3500	4000	4500	5000
ρ, g/cm^3	2.55−9	1.16−6	3.86−5	5.75−4	4.16−3	1.84−2	5.74−2
P, atm	1.32−5	6.80−3	2.64−1	4.40+0	3.62+1	1.78+2	6.15+2

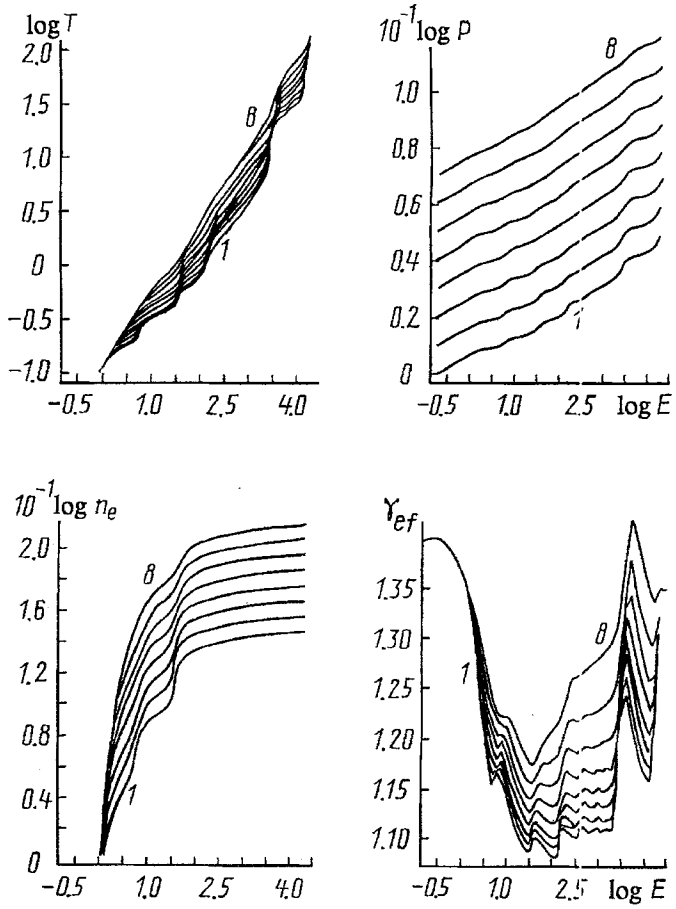

Fig. 3. Dependence of thermodynamic characteristics of air on E and ρ. log E, kJ/g.

the electron concentration at low temperatures: they are NO^+ in air and the Martian atmosphere, O_2^+ in water vapor, and SiO^+ in silicon dioxide.

Figure 2 presents temperature dependences of pressure, specific internal energy, electron concentration, and effective adiabatic exponent for silicon dioxide for a set of densities. The same figure presents the curve equilibrium between SiO_2 vapor and condensed phase. Dependences of the density and pressure of the saturated vapor on the temperature for SiO_2 are presented in Table 2.

Representation of data as a function of the variables ρ, E is frequently required in gasdynamic applications. Interpolation of results on the plane of new variables leads to loss of precision, especially within regions corresponding to pauses in dissociation and ionization, and therefore thermophysical properties of matter were tabulated as dependences on both $\rho-T$ variables and $\rho-E$ variables. Figure 3 demonstrates their behavior for air as a function of E for predetermined ρ. Curves 1-8 in Figs. 2 and 3 correspond to $\delta = 10^{-6}-10^{1}$ in intervals of one order.

It should be noted that the equations of chemical equilibrium were solved using the equilibration method, and the concentrations of small components were calculated directly using equilibrium constants. Solution of the Saha system in the absence of molecules was carried out using an iteration method [29], where the temperature and the electron density were chosen as independent variables.

TABLE 3. States of N and O Atoms and Their Ions with Tabulated Photoionization Cross Sections

Ion	Term	Term of the residual ion	Ion	Term	Term of the residual ion
N I			O I		
1	$2s^2 2p^3\ ^4S$	$2s^2 2p^2\ ^3P$	1	$2s^2 2p^4\ ^3P$	$2s^2 2p^3\ ^4S,\ ^2P,\ ^2D$
2	$2s^2 2p^3\ ^2D$	$2s^2 2p^2\ ^3P,\ ^1D$	2	$2s^2 2p^4\ ^1D$	$2s^2 2p^3\ ^2P,\ ^2D$
3	$2s^2 2p^3\ ^2P$	$2s^2 2p^2\ ^3P,\ ^1D,\ ^1S$	3	$2s^2 2p^4\ ^1S$	$2s^2 2p^3\ ^2P$
N II			O II		
1	$2s^2 2p^2\ ^3P$	$2s^2 2p\ ^2P$	1	$2s^2 2p^3\ ^4S$	$2s^2 2p^2\ ^3P$
2	$2s^2 2p^2\ ^1D$	$2s^2 2p\ ^2P$	2	$2s^2 2p^3\ ^2D$	$2s^2 2p^2\ ^3P,\ ^1D$
3	$2s^2 2p^2\ ^1S$	$2s^2 2p\ ^2P$	3	$2s^2 2p^3\ ^2P$	$2s^2 2p^2\ ^1S,\ ^3P,\ ^1D$
N III			O III		
1	$2s^2 2p\ ^2P$	$2s^2\ ^1S$	1	$2s^2 2p^2\ ^3P$	$2s^2 2p\ ^2P$
2	$2s2p^2\ ^4P$	$2s2p\ ^3P$	2	$2s^2 2p^2\ ^1D$	$2s^2 2p\ ^2P$
3	$2s2p^2\ ^2D$	$2s2p\ ^3P,\ ^1P$	3	$2s^2 2p^2\ ^1S$	$2s^2 2p\ ^2P$
N IV			O IV		
1	$2s^2\ ^1S$	$2s\ ^2S$	1	$2s^2 2p\ ^2P$	$2s^2\ ^1S$
2	$2s2p\ ^3P$	$2s\ ^2S$	2	$2s2p^2\ ^4P$	$2s2p\ ^3P$
3	$2s2p\ ^1P$	$2s\ ^2S$	3	$2s2p^2\ ^2D$	$2s2p\ ^3P$
N V			O V		
1	$2s\ ^2S$	$1s^2\ ^1S$	1	$2s^2\ ^1S$	$2s\ ^2S$
2S2	$2p\ ^2P$	$1s^2\ ^1S$	2	$2s2p\ ^3P$	$2s\ ^2S$
N VI			3	$2s2p\ ^1P$	$2s\ ^2S$
1	$1s^2\ ^1S$	$1s\ ^2S$	O VI		
O VII			1	$2s\ ^2S$	$1s^2\ ^1S$
1	$1s^2\ ^1S$	$1s\ ^2S$	2	$2p\ ^2P$	$1s^2\ ^1S$

Optical Properties. Calculation of spectral absorption coefficients involves summing up contributions of a large number of components and taking into account numerous transitions, and each of the transitions can play a leading role at a certain temperature within a certain spectral region. The main mechanisms responsible for absorption of radiation in gases and plasmas are the processes of braking absorption in the fields of ions, atoms, and molecules, photoionization from the ground and excited states of atoms and ions, absorption in the processes of photoionization and photodissociation of molecules, photoionization of internal electron shells of particles, absorption in vibronic molecular transitions, and absorption in spectral lines of atoms and ions. The magnitude of absorption in the specified processes was calculated within the following approximations.

The absorption cross section in free-free transitions in the field of a neutral particle was expressed in terms of the cross section σ_0 of elastic scattering of an electron on the particle. To describe the atomic absorption the following formula obtained in [30] was used:

$$\sigma^{ff}(\varepsilon) = \frac{16\sqrt{2}}{3\sqrt{\pi}}\,\alpha\,\pi\,a_0^3\sigma_0\left(\frac{Ry}{\varepsilon}\right)^{3/2}\left(\frac{\varepsilon}{2kT}\right)^{1/2}\exp\left(\frac{\varepsilon}{2kT}\right)K_2\left(\frac{\varepsilon}{2kT}\right). \tag{10}$$

Here $\alpha = 2\pi e^2/hc$, a_0 is the Bohr radius, $K_2(x)$ is a Bessel function of imaginary argument. The braking absorption on molecules was determined according to [31, 32]:

$$\sigma^{ff}(\varepsilon) = 32\,\frac{\sqrt{2}}{\sqrt{\pi}}\,\alpha\,a_0\,\pi\,a_0^2\sigma_0\left(\frac{Ry}{\varepsilon}\right)^3\left(\frac{kT}{Ry}\right)^{3/2}\left(1+\frac{3\varepsilon}{4kT}\right). \tag{11}$$

The absorption cross section in the scattering of an electron on an ion was described using the Kramers formula with the Gaunt correcting multiplier:

$$\sigma^{ff}(\varepsilon) = \frac{256\sqrt{\pi}}{3\sqrt{3}} \alpha a_0 (\pi a_0^2)^2 i^2 \left(\frac{Ry}{kT}\right)^{1/2} \left(\frac{Ry}{\varepsilon}\right)^3 G(T, \varepsilon), \tag{12}$$

where i is the ionic charge, and G is the Gaunt correction factor [33].

Cross sections of bound-free transitions were calculated within various approximations. For atoms and ions of N and O in the ground state and low-lying levels they were found according to the Hartree-Fock method [34]. Table 3 presents a list of states for which the corresponding cross sections were tabulated.

Absorption cross sections of hydrogen and H-like ions were calculated using the exact formulas [35] for $n \leq 4$. For C, Si, and their ions cross sections for all levels weredetermined using the quantum defect method [36]:

$$\sigma_{nl}^{bf}(\varepsilon) = \frac{4\alpha}{3} \pi a_0^2 \left(\frac{\varepsilon}{Ry}\right) \left(\frac{Ry}{p_{nl}}\right)^2 \sum_{l'=l\pm1} C_{l'} |g_{ll'}|^2, \tag{13}$$

where $p_{nl} = Z^2 Ry / n_l^{*2}$ is the binding energy of an electron at the level nl; $C_{l'}$ is a factor that depends on the spin and the orbital moment of the system in the ground and final excited states; the function g is related to the radial integral. Cross sections of photoionization of all particles from excited states with a principal quantum number n greater than that for the ground state of the outer electron were also calculated using the quantum defect method. For levels with a low binding energy and levels with an orbital number $l \geq 3$ the hydrogenlike approximation was used:

$$\sigma_{nl}^{bf}(\varepsilon) = \frac{64}{3\sqrt{3}} \alpha \pi a_0^2 \frac{p_{nl}^2 Ry}{n\varepsilon^3}. \tag{14}$$

To determine photoionization cross sections of internal electronic shells of atoms and ions the Hartree-Fock-Slater method [37] was used.

In calculations of photoionization of the molecules H_2, CO, C_2, and CN we used a stepwise approximation based on experimental data [38, 39]:

$$\sigma^{bf}(\varepsilon) = \begin{cases} 0, & \varepsilon < \varepsilon_p, \\ \sigma_p, & \varepsilon \geq \varepsilon_p. \end{cases} \tag{15}$$

The parameters ε_p and σ_p (10^{-18}) are presented in Table 4. Photoionization cross sections of N_2, O_2, and NO were determined according to data from [40] obtained at NTP. Averaging them gives the following expressions (ε, eV; σ, 10^{-18} cm^2) [39]:

$$\sigma_{N_2} = \begin{cases} 2.5 + 338.416\,(\varepsilon^{-1} - 1), & 16.487 < \varepsilon \leq 61.980, \\ 17.5 \exp\,[-298.75\,(\varepsilon^{-1} - 0.0605)\,], & 14.750 < \varepsilon \leq 16.487, \\ 1, & 12.396 < \varepsilon \leq 14.750, \end{cases}$$

$$\sigma_{O_2} = \begin{cases} 30, & 15.495 < \varepsilon \leq 26.400, \\ 7, & 14.578 < \varepsilon \leq 15.495, \\ 10 \exp\,[-142.56\,(\varepsilon^{-1} - 0.06857)\,], & 11.806 < \varepsilon \leq 14.578, \\ 0.3, & 9.669 < \varepsilon \leq 11.806, \end{cases} \tag{16}$$

$$\sigma_{NO} = \begin{cases} 7.5 + 387.80\,(\varepsilon^{-1} - 0.016134), & 20.676 < \varepsilon \leq 61.980, \\ 20 - 1053.75\,(\varepsilon^{-1} - 0.048402), & 15.495 < \varepsilon \leq 20.676, \\ 3.0 + 1756.5\,(\varepsilon^{-1} - 0.06454), & 13.475 < \varepsilon \leq 15.495, \\ 20 \exp\,[-97.72\,(\varepsilon^{-1} - 0.07422)\,], & 10.326 < \varepsilon \leq 13.475, \\ 2.2, & 8.729 < \varepsilon \leq 10.326. \end{cases}$$

TABLE 4. Parameters of Photoionization Cross Sections of Molecules

Parameter	H_2	CO	C_2	CN
ε_p, eV	15.43	14.22	12.00	14.61
$\sigma_p\,(10^{-18})$, cm^2	7.00	15.00	10.00	5.00

Within the harder region of the spectrum the cross sections of molecular absorption were calculated using atomic cross sections under the assumption of their additivity [41].

The absorption cross section in the photodissociation process can be represented as follows [42]:

$$\sigma^{bf}(\varepsilon) = \frac{1}{3}\pi a_0^2 \alpha^2 \left(\frac{\varepsilon}{Ry}\right) R_e^2(\varepsilon) \sum_{v',v''} W_{v''}(T)\, q_{v''}(\varepsilon)\, \varphi(\varepsilon - \varepsilon_{v',v''}), \tag{17}$$

where $W_{v''}$ is the Boltzmann probability for a particle to be at the level v''; $q_{v''}$ is the Franck-Condon factor for transitions between vibrational levels of the neutral molecule and the residual ion; R_e^2 (a.u.) is the electronic part of the transition dipole moment; φ accounts for the presence of a threshold for the $v'' - v'$ transition and its frequency dependence. In these calculations simple cross-section approximations were used, for example, for the O_2 molecule [40]:

$$\sigma_{O_2} = \begin{cases} 0.4, & 9.456 < \varepsilon \le 9.745, \\ 2.2, & 9.238 < \varepsilon \le 9.456, \\ 7.0, & 9.036 < \varepsilon \le 9.238, \\ 12.0, & 8.160 < \varepsilon \le 9.036, \\ 12 \exp\left[-189.66\,(\varepsilon^{-1} - 0.1225)\right], & 7.083 < \varepsilon \le 8.160. \end{cases} \tag{18}$$

In calculations of absorption in spectral lines of atoms and ions their contour was given as a Voigtian (in this case the electronic collisional broadening and the thermal Doppler effect were taken into account):

$$\sigma_{ij}^{bb}(\varepsilon) = \frac{\pi e^2 h}{mc} f_{ij}\, \varphi(\varepsilon), \tag{19}$$

$$\varphi(\varepsilon) = \frac{1}{\sqrt{\pi}\,\Delta\varepsilon_D} H(a, u), \quad H(a, u) = \frac{a}{\pi} \int_{-\infty}^{+\infty} \frac{\exp(-y^2)\,dy}{a^2 + (u - y)^2}. \tag{20}$$

Here f_{ij} is the transition oscillator strength, $a = \gamma_e / 2\Delta\varepsilon_D$ is the ratio of the collisional halfwidth to the Doppler one $\Delta\varepsilon_D = \varepsilon_0 (2kT/Mc^2)^{1/2}$, $u = (\varepsilon - \varepsilon_0)/\Delta\varepsilon_D$. The electronic halfwidth of lines (cm^{-1}) was determined according to [43]:

for neutrals

$$\frac{\gamma_{ij}}{2} = 11.4 \left(\frac{8kT}{\pi m}\right)^{1/6} n_e C_4^{2/3}, \quad C_4^{ij} = \frac{2\pi e^2}{3h^2} \sum_l \left[\frac{S_{il}}{g_i \omega_{il}} + \frac{S_{jl}}{g_j \omega_{jl}}\right], \tag{21}$$

for ions

$$\frac{\gamma_{ij}}{2} = 8 \left(\frac{\pi}{3}\right)^{3/2} \frac{h a_0}{2\pi m} \left(\frac{Ry}{kT}\right)^{1/2} n_e \left[\sum_l |\langle i | \bar{r} | l \rangle|^2 g\left(\frac{3kT}{2 | E_i - E_l |}\right) + \sum_l |\langle j | \bar{r} | l \rangle|^2 g\left(\frac{3kT}{2 | E_j - E_l |}\right)\right]. \tag{22}$$

All dipole transitions from the initial i and final j states contribute to the broadening.

TABLE 5. Number of Discrete Levels and Lines of Components of Air

Ion		1	2	3	4	5	8	7	8
N	levels	18	21	32	20	12	18	10	
	lines	37	78	54	51	83	125	45	
O	levels	16	35	40	27	30	12	18	10
	lines	37	59	61	61	55	83	125	45
Ion		1-14			15		16	17	18
Ar	levels	1			30		25	22	10
	lines	1			66		42	46	45

Data on the number of levels and lines individually taken into account for various components of the air plasma are presented in Table 5. It should be noted that in the calculations air was given as a gaseous mixture with the following volume ratio of the components: N_2 – 0.7812, O_2 – 0.2095, Ar – 0.0093. Since argon contributes noticeably to absorption only at high temperatures when N and O are completely ionized, only its multi-charge ions were included in the computations. This table gives an idea of the number of transitions in the continuous and discrete spectra included in the present computations.

Absorption cross sections of vibronic transitions of diatomic molecules were determined using an approximate method that employs an expression for the integral absorption in the vibronic band (per particle) [44]

$$k^{bb}(\nu) = \frac{4\pi}{3}\pi a_0^2 \alpha \frac{kTq_{v'v''}}{Q(T)B_{v''}}\nu S_e \exp\left(-\frac{E_{e''}+E_{v''}}{kT}\right)\left[1-\exp\left(-\frac{h\nu}{kT}\right)\right]. \quad (23)$$

Here $B_{v''}$ is the rotational constant of the lower level, $q_{v'v''}$ is the Franck-Condon factor, $Q(T)$ is the statistical sum over the internal degrees of freedom of the molecule, S_e (a.u.) is the strength of the electronic transition, ν (sec^{-1}) is the frequency. Dividing (23) by the width of the vibrational band $\Delta\nu = (\nu_{e'} + \nu_{e''})/2$, we obtain the absorption cross section averaged over the $v'v''$ band. The following vibronic bands of diatomic molecules were taken into account:

O_2 – Schumann-Runge
N_2 – first positive
– second positive
– Birdge-Hopfield 1
– Birdge-Hopfield 2
– Lyman-Birdge-Hopfield
NO – β
– γ
– δ
– ε
– ε'
N_2^+ – Mainell
– first negative
SiO – violet
C_2 – Swan
– Mullican
– Delander-Azambja
– Fox-Herzberg
– Freimark
CO – fourth positive
– Angstrom
CO^+ – comet tail
– first negative
CN – fundamental red
– violet
OH – violet
H_2 – second Lyman
– second Werner

All necessary data were taken from [26, 32, 39, 45].

To calculate the contribution of triatomic CO_2 and H_2O molecules to the absorption we used experimental information on cold absorption coefficients [46, 47] and data on temperature dependences of cross sections within separate spectral ranges [48, 49]. Due to lack of data, the absorption of SiO_2 was not taken into account (in addition, its concentration in the vapor phase is negligible).

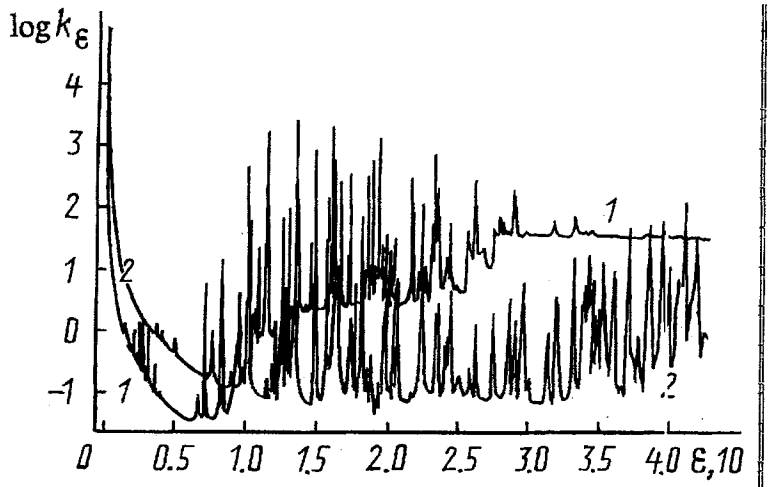

Fig. 4. Absorption coefficients of air at $\delta = 10^{-1}$: 1) $T = 3 \cdot 10^4$ K; 2) 10^5 K. log k_ε, cm^{-1}; $10^{-1}\varepsilon$, eV.

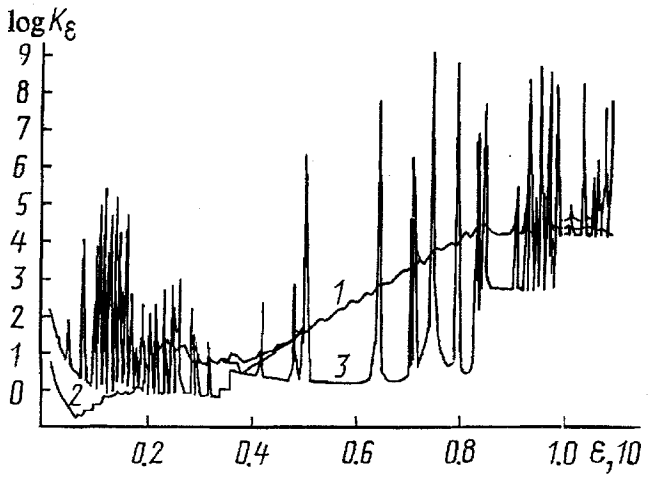

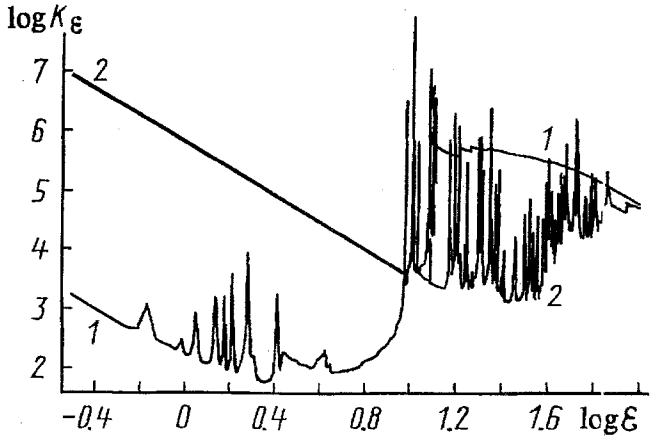

Fig. 5. Absorption coefficient of the Martian atmosphere, $T = 8 \cdot 10^3$ K, $\delta = 10^{-2}$. log K_ε, cm^2/g; $10^{-1}\varepsilon$, eV

Fig. 6. Absorption coefficient of water, $\delta = 10^0$: 1) $T = 1$ eV; 2) 10 eV.

Let us consider the results obtained (more detailed information on the absorption coefficients of plasmas of the media under consideration is presented in [50]). Figure 4 shows the dependence of the absorption coefficient of air on the energy of a quantum within the range of states where it is determined by radiative transitions in atoms and ions, whereas the role of molecules can be neglected. It is clear that the absorption resulting from transitions of electrons of the optical shell increases with temperature for quanta with low energies and decreases for high-energy quanta.

Results of calculations of the absorption coefficient of the Martian atmosphere are presented in Fig. 5. Here at $T = 8 \cdot 10^3$ K and $\delta = 10^{-2}$ the contributions of molecular components (curve 2) and atoms and ions (curve 3) to the value of the total absorption coefficient (curve 1) are presented. It is clear that the absorption level at $\varepsilon > 2$ eV determines the molecular absorption far from spectral lines. It should be noted that here the weight absorption coefficient $K_e = k_e/\rho$ is presented. This quantity is frequently used in the solution of problems of radiation gas dynamics instead of the linear absorption coefficient, since it depends weakly on density, which is convenient for interpolation of spectral parameters over ρ.

The example of the absorption spectrum of water is presented in Fig. 6, where the weight coefficient for the temperatures $T = 1$ and 3.16 eV and the density $\delta = 10^0$ was calculated on the energy scale described above.

Results of calculations of spectrally integrated mean Planck absorption coefficients and Rosseland radiation paths in air and silicon dioxide are presented in Fig. 7. Curves 1-15 correspond to the relative densities $\delta =$

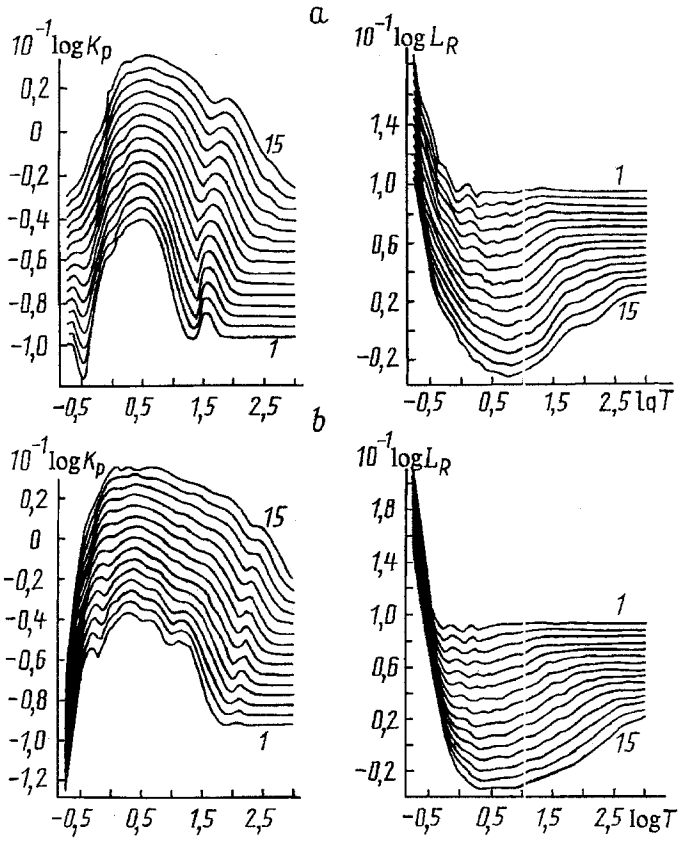

Fig. 7. Planck and Rosseland averages for air (a) and SiO_2 (b). K_P, cm^{-1}; L_R, cm.

$10^{-6}-10^{1}$ in intervals of half an order. It should be noted that in these calculations the scattering of radiation on free electrons is taken into account, which bounds the values of mean quantities at high temperatures (when total ionization is achieved) and at low densities:

$$K_P = \frac{15}{\pi^4}\int_0^\infty k_f(x)\,\frac{x^3 e^{-x}}{1-e^{-x}}\,dx, \quad L_R = \frac{15}{4\pi^4}\int_0^\infty \frac{dx}{k_f(x)}\,\frac{x^4 e^{-x}}{(1-e^{-x})^2}. \tag{24}$$

where $k_f = k(x) + k_s$, $k(x) = k(\varepsilon/T)$ is the absorption coefficient, and the scattering coefficient k_s is as follows:

$$k_s = \frac{8\pi}{3} a_0^2 \alpha^4 n_e. \tag{25}$$

Let us briefly discuss the limits of applicability of the results obtained. On the side of high densities these data are bounded by manifestation of the effects of nonideality [51, 52] (at temperatures $T \sim 1$ eV and densities $\delta \sim 1$ the quantity $\gamma \sim 1$). Under these conditions the calculation of thermodynamic properties and composition within the annular Debye approximation can be considered to be an extrapolation to the region of strong nonideality. Within the rest of the $T-\delta$ region the approximation being used is rather applicable.

The effects of nonideality also exert the optical properties of plasma, resulting in broadening, confluence, and transition to the continuous spectrum of a portion of the excited levels of the discrete spectrum. In addition, under the effect of the plasma microfield the probability of realization of some states is decreased [23]. The first effect leads to a shift in the photoionization thresholds toward lower energies and increases, on average, the absorption coefficient by a factor of exp $(h\Delta\nu/kT)$. The second effect results in a decrease in absorption within the longwave region due to a decrease in the contribution of the photoionization of nonrealized levels. Although these effects lead to deviation of the spectrum from the ideal one within various ranges of energy of the quanta, the first effect is neutralized by the second since lines that are broadened and transferred to the continuum and lie near the photoionization threshold turn out not to be realized. Braking processes, in turn, contribute substantially to the

absorption of quanta with energy $\varepsilon < T$, and therefore nonrealization of levels does not play a leading part in this case. In addition, this is not the most important region of the spectrum in radiation transfer. The considerations presented and the lack of a reliable theory of the effects of nonideality on the optical properties of plasma [52] served as arguments in favor of calculating these parameters without accounting for nonideality.

Conclusion. As a result of the investigations carried out a databank on opticophysical properties of matter within the region of temperatures from 0.1 to 10^3 eV and densities of $10^{-9}-10^{-2}$ g/cm^3 is composed. It includes the following characteristics:

1. Component composition and thermodynamic properties of air, water, silicon dioxide, and the Martian atmosphere.
2. Spectral coefficients of continuous absorption. They are determined on a floating energy scale that contains the absorption thresholds of the components present in the gas. These data make it possible to average spectra over arbitrary spectral regions.
3. Integral absorption in the lines at given T and ρ, and broadening constants. Such information is necessary for taking into account the contribution of lines to the total absorption upon averaging over the ranges.
4. Total spectral absorption coefficients, which make it possible to resolve individual features of the spectrum.
5. Total small-group absorption coefficients within the range of the energy of quanta of $10^{-1}-10^4$ eV (1941 spectral groups).
6. Group-averaged absorption coefficients. Information in item 5 makes it possible to calculate these values easily for any division into groups.
7. Planck- and Rosseland-averaged group and integral absorption coefficients and mean free paths.
8. Data on cross sections of individual components within the region of their existence, which makes it possible to analyze their role as a function of temperature, density, and the portion of the spectrum.

The authors are grateful to the Soros Foundation for support for the present work.

NOTATION

ρ, density; T, temperature; P, pressure; E, specific internal energy; γ_{ef}, effective adiabatic exponent; n, concentration of particles; δ, relative density; γ and Γ, nonideality parameters; r_D, Debye radius; Σ_i, statistical sum; g_{ij} and g_i, statistical weights of a level; I_i, ionization potential; ΔI_i, decrease in the ionization potential; E_{ij} and E_i, energy of a level; A_i, molecular weight; P_k and E_k, Coulomb corrections to pressure and internal energy; $h\omega_\nu$, energy of the vibrational quantum of a molecule; ε, energy of a quantum; α, fine-structure constant; ν, frequency of a quantum; S_{ij} and ω_{ij}, transition strength and circular frequency; γ_{ij}, line width; k_ε, linear spectral absorption coefficient; K_ε, weight absorption coefficient; K_P and K_R, Planck mean absorption coefficient and Rosseland mean free path.

REFERENCES

1. V. A. Bronshten, Physics of Meteorite Phenomena [in Russian], Moscow (1976).
2. S. S. Grigoryan and G. S. Shapiro (eds.), Action of a Nuclear Explosion, Collection of Translated Papers [in Russian], Moscow (1971).
3. V. N. Nikolaevskii (ed.), High-Speed Shock Phenomena, Collection of Translated Papers [in Russian], Moscow (1973).
4. S. I. Anisimov, Ya. A. Imas, G. S. Romanov, and Yu. S. Khodyko, Action of High-Power Radiation on Metals [in Russian], Moscow (1970).
5. Yu. P. Raizer, Laser Spark and Discharge Propagation [in Russian], Moscow (1974).
6. V. A. Burtsev, N. V. Kalinin, and A. V. Luchinskii, Electric Explosion of Conductors and Its Applications in Electrophysical Installations [in Russian], Moscow (1990).
7. N. M. Kuznetsov, Thermodynamic Functions and Shock Adiabats of Air [in Russian], Moscow (1965).

8. R. K. M. Landshoff and J. L. Magee, Thermal Radiation Phenomena, Vols. 1, 2, New York (1969).
9. I. V. Avilova, L. M. Bibernam, V. S. Vorob'yov, et al., Optical Properties of Hot Air [in Russian], Moscow (1970).
10. G. A. Kobzev, Optical Properties of Air Plasma at High Temperatures, Preprint of IVTAN, No. 1-112, Moscow (1983).
11. G. A. Kobzev and V. A. Nuzhnyi, Spectral and Integral Characteristics of the Continuous Spectrum of Air Plasma at High Temperatures, Preprint of IVTAN, No. 1-131, Moscow (1984).
12. G. A. Kobzev and V. A. Nuzhnyi, Optical Properties of Air Plasma with Account for Spectral Lines, T = 20,000–30,000 K, Preprint of IVTAN, No. 1-134, Moscow (1984).
13. N. N. Kalitkin, L. V. Kuz'mina, and V. S. Rogov, Tables of Thermodynamic Functions and Transport Coefficients of Plasma [in Russian], Moscow (1972).
14. B. V. Zamyshlyaev, E. L. Stupitskii, A. G. Guz', et al., Composition and Thermodynamic Functions of Plasma [in Russian], Moscow (1984).
15. V. K. Gryaznov, I. L. Iosilevskii, Yu. G. Krasnikov, et al., Thermophysical Properties of Working Media of a Gas-Phase Nuclear Reactor [in Russian], Moscow (1980).
16. G. S. Romanov, L. K. Stanchits, and K. L. Stepanov, Tables of Group-Averaged Absorption Coefficients of Aluminum Plasma, Minsk (1984), Deposited at BelVINITI No. 837Be-D84.
17. F. N. Borovik, S. I. Kas'kova, G. S. Romanov, et al., Zh. Prikl. Spektr., **39**, No. 6, 923-929 (1983).
18. Yu. S. Boiko, Yu. M. Grishin, A. S. Kamrukov, et al., Thermodynamic and Optical Properties of Plasma of Metals and Dielectrics [in Russian], Moscow (1988).
19. S. S. Katsnel'son and G. A. Koval'skaya, Thermophysical and Optical Properties of Argon Plasma [in Russian], Novosibirsk (1985).
20. F. N. Borovik, S. I. Kas'kova, G. S. Romanov, et al., Equation of State and Absorption Coefficients of Xenon Plasma, Part I, Moscow (1982), Deposited at VINITI, No. 6022; Part II, Moscow (1982), Deposited at VINITI, No. 6023.
21. Yu. S. Boiko, Yu. M. Grishin, A. S. Kamrukov, et al., Thermophysical and Optical Properties of Ionized Gases at Temperatures up to 100 eV [in Russian], Moscow (1988).
22. V. I. Derzhiev, A. G. Zhidkov, and S. I. Yakovlenko, Emission from Ions in Nonequilibrium Dense Plasma [in Russian], Moscow (1986).
23. V. E. Fortov and I. T. Yakubov, Physics of Imperfect Plasma [in Russian], Chernogolovka (1982).
24. L. V. Gurvich, I. V. Veits, V. A. Medvedev, et al. (eds.), Thermodynamic Properties of Individual Substances: Handbook [in Russian], Moscow (1980).
25. A. A. Radtsig and B. M. Smirnov, Handbook on Atomic and Molecular Physics [in Russian], Moscow (1980).
26. K. P. Huber and G. Herzberg, Molecular Spectra and Molecular Structure. IV. Constants of Diatomic Molecules [Russian translation], Moscow (1984).
27. C. Moore, Atomic Energy Levels, Vols. 1, 2, Washington (1949).
28. Thermophysical Properties of Chemically Reacting Heterogeneous Mixtures, Proc. of ENIN, Issue 7, Moscow (1973).
29. G. S. Romanov and L. K. Stanchits, Dokl. Akad. Nauk BSSR, **15**, No. 3, 204-205 (1971).
30. V. A. Kas'yanov and A. N. Starostin, Zh. Eksp. Teor. Fiz., **48**, Issue 1, 295-302 (1965).
31. O. B. Firsov and M. I. Chibisov, Zh. Eksp. Teor. Fiz., **39**, Issue 6(12), 1770-1776 (1960).
32. V. A. Kamenshchikov, Yu. A. Plastinin, and V. M. Nikolaev, Radiation Properties of Gases at High Temperatures [in Russian], Moscow (1971).
33. J. R. Stallcop and K. W. Billman, Plasma Phys., **16**, 1187-1189 (1974).
34. S. I. Kas'kova, G. S. Romanov, K. L. Stepanov, et al., Abstracts of the 1st All-Union Symposium on Radiation Plasmadynamics, Moscow (1989).
35. H. Bethe and E. Salpeter, Quantum Mechanics of One- and Two-Electron Atoms [Russian translation], Moscow (1960).
36. A. Burgess and M. J. Seaton, Mon. Not. Roy. Astron. Soc., **120**, No. 2, 121-151 (1960).

37. F. N. Borovik, G. S. Romanov, and K. L. Stepanov, Cross Sections of Continuous Absorption of Multi-Ionized Plasma of Carbon, Moscow (1981), Deposited at VINITI, No. 4912.
38. V. P. Stulov and V. N. Mirskii, Flow at the Front Surface of a Body upon Intense Evaporation under the Effect of Radiative Heating, Report No. 1416 of the Institute of Mechanics of Moscow State University, Moscow (1972).
39. S. T. Surzhikov, Computational Models of Radiation and Gasdynamic Processes in Low-Temperature Plasma, D. Sci. Thesis, Moscow (1990).
40. K. Watanabe, Investigations of the Upper Atmosphere Using Rockets and Satellites [Russian translation], Moscow, 280-358 (1961).
41. B. E. Cole and R. N. Dexter, JQSRT, **19**, 467-471 (1978).
42. A. Kh. Mnatsakyan, Teplofiz. Vys. Temp., **6**, No. 2, 236-241 (1968).
43. H. R. Griem, Spectral Line Broadening in Plasmas [Russian translation], Moscow (1978).
44. L. A. Kuznetsova, N. E. Kuz'menko, Yu. Ya. Kuzyakov, et al., Probabilities of Optical Transitions in Diatomic Molecules [in Russian], Moscow (1980).
45. Yu. A. Plastinin and G. G. Baula, Studies in Physical Gas Dynamics [in Russian], Moscow, 41-61 (1966).
46. G. Herzberg, Molecular Spectra and Molecular Structure. III. Electronic Spectra and Electronic Structure of Polyatomic Molecules [Russian translation], Moscow (1969).
47. H. Okabe, Photochemistry of Small Molecules [Russian translation], Moscow (1981).
48. A. P. Zuev and A. Yu. Starikovskii, Zh. Prikl. Spektr., **52**, No. 3, 455-465 (1990).
49. N. I. Moskalenko, Yu. A. Il'in, and N. K. Pokotilo, Zh. Prikl. Spektr., **34**, No. 3, 475-480 (1981).
50. G. S. Romanov, Yu. A. Stankevich, L. K. Stanchits, and K. L. Stepanov, Thermodynamic Properties, Spectral and Averaged Absorption Coefficients of Multicomponent Gases within a Wide Range of Parameters, Preprint No. 2 of the Institute of Heat and Mass Transfer, Minsk (1993).
51. L. M. Biberman and G. E. Norman, Uspekhi Fizicheskikh Nauk, **91**, No. 2, 193-246 (1967).
52. G. E. Norman, A. A. Valuev, and A. S. Kaklyugin, Radiation Plasmadynamics [in Russian], Vol. 1, Moscow, 396-437 (1991).